Surface Science 603 (2009) 3136–3144

Contents lists available at ScienceDirect

Surface Science

journal homepage: www.elsevier.com/locate/susc

Adsorption and decomposition of NO on O-covered planar and faceted Ir(2 1 0)

Wenhua Chen [a,*], Alan L. Stottlemyer [b], Jingguang G. Chen [b], Payam Kaghazchi [c], Timo Jacob [c,d], Theodore E. Madey [a,1], Robert A. Bartynski [a]

[a] Department of Physics and Astronomy, and Laboratory for Surface Modification, Rutgers, The State University of New Jersey, Piscataway, NJ 08854, United States
[b] Center for Catalytic Science and Technology, University of Delaware, Newark, DE 19716, United States
[c] Fritz-Haber-Institut der Max-Planck-Gesellschaft, Faradayweg 4-6, D-14 195 Berlin-Dahlem, Germany
[d] Theoretische Elektrochemie, Universität Ulm, Albert-Einstein-Allee 47, D-89 069 Ulm, Germany

ARTICLE INFO

Article history:
Received 14 July 2009
Accepted for publication 27 August 2009
Available online 2 September 2009

Keywords:
Iridium
Faceting
Nitric oxide
Oxygen
Adsorption
Decomposition

ABSTRACT

We report on the adsorption and decomposition of NO on O-covered planar Ir(2 1 0) and nanofaceted Ir(2 1 0) with variable facet sizes investigated using temperature programmed desorption (TPD), high-resolution electron energy loss spectroscopy (HREELS), and density functional theory (DFT). When pre-covered with up to 0.5 ML O, both planar and faceted Ir(2 1 0) exhibit unexpectedly high reactivity for NO decomposition. Upon increasing the oxygen coverage to 0.7 ML O, planar Ir(2 1 0) has little activity while faceted Ir(2 1 0) still remains active toward NO decomposition, although NO decomposition is completely inhibited when both surfaces are pre-covered by 1 ML O. NO molecularly adsorbs on O-covered Ir at 300 K. At low NO and oxygen coverage, NO adsorbs on the atop sites of planar Ir(2 1 0) while on the bridge and atop sites of faceted Ir(2 1 0) composed of (1 1 0) and {3 1 1} faces. No evidence for size effects in the decomposition of NO on O-covered faceted Ir(2 1 0) is observed for average facet size in the range 5–14 nm. Our findings should be of importance for development of Ir-based catalysts for NO decomposition under oxygen-rich conditions.

1. Introduction

Catalytic conversion of NO to N_2 under oxygen-rich conditions has received increasing attention due to the challenge for future new exhaust catalysts needed for current diesel and lean-burn engines [1–6], which operate under high oxygen concentrations that poison most platinum group metal catalysts. Of particular interest is the selective catalytic reduction (SCR) of NO by hydrocarbons (HCs) in the presence of excess oxygen, which is believed to be the most promising approach for the removal of NO [7]. It has been shown that Pt- and Ir-based catalysts are the most active among noble metals for SCR of NO by HCs [4] and Ir is more active and selective than Pt at higher temperatures [3]. However, the SCR of NO by HCs leads to the formation of secondary pollutants such as oxygenated HCs, CO and N_2O. The direct decomposition of NO without using any reductant can avoid these secondary pollutants with the exception of N_2O, which is probably the most attractive solution in pollution control [7].

The adsorption and decomposition of NO in the presence of pre-adsorbed oxygen have been studied both experimentally and theoretically on many metal surfaces such as Pd [8], Pt [9,10], Rh [11–14], Ru [15], Ir [16,17], and Ni [18,19]. In general, with pre-adsorbed oxygen the surface becomes less active for NO dissociation. The reduced reactivity of the surface is most likely governed by the reduced degree of backbonding between the local d-band of the metal and the $2\pi^*$ antibonding orbital of NO due to electrons withdrawn from the metal by pre-adsorbed oxygen [14,18]. As the pre-adsorbed oxygen coverage increases, the degree of backbonding and thus electron density in the $2\pi^*$ antibonding orbital of NO reduces, leading to a higher activation barrier for NO dissociation [14,18]. Nevertheless, when comparing the activation barrier for NO dissociation on Rh with different surface structures pre-covered with oxygen, it has been found that steric effects exceed electronic effects [14], i.e. the local geometrical structure of the surface plays a key role in determining the activation barrier for NO dissociation.

An industrial catalyst is typically in the form of small metal particles on the nanometer scale highly dispersed over an oxide support, which usually has wide distribution of the metal particle sizes and shapes. In studies of supported metal catalysts, it has been shown that metallic particle size, shape and structure as well as support all influence their catalytic performance. In order to achieve a fundamental understanding of the reaction mechanism, planar surfaces of metal single crystals or metallic nanoclusters grown on such surfaces are often used as model systems. Following

* Corresponding author.
E-mail address: wchen@physics.rutgers.edu (W. Chen).
[1] In memory of Prof. Theodore E. Madey who passed away on July 27, 2008 at the age of 70.

0039-6028/$ - see front matter © 2009 Elsevier B.V. All rights reserved.
doi:10.1016/j.susc.2009.08.027

this approach, we use metallic single crystals to reproducibly prepare in situ model surfaces with different surface morphologies, ranging from planar surfaces to nanometer-scale faceted surfaces with well-defined structure and controlled size, free of any support material. The faceted surfaces serve as model catalysts to bridge the gap between the planar surfaces of metal single crystals and supported metal nanoparticles.

In this work, an Ir(2 1 0) crystal was used to prepare planar or faceted Ir(2 1 0) with tunable facet size between 5 and 14 nm, which then were used to investigate the effects of pre-adsorbed oxygen on adsorption and decomposition of NO. Planar Ir(2 1 0) is an atomically rough surface with four layers exposed [20], while faceted Ir(2 1 0) is composed of three-sided nanoscale pyramids exposing one (1 1 0) face and two {3 1 1} faces on each pyramid [21,22]. The fabrication of clean planar and faceted Ir(2 1 0) enables exploration of structure sensitivity and size effects in NO decomposition on O-covered unsupported Ir. The well-defined crystallographic orientation of the facets allows for detailed experimental and theoretical characterization of not only planar Ir(2 1 0) but also faceted Ir(2 1 0). A combination of temperature programmed desorption (TPD), high resolution electron loss spectroscopy (HREELS) and density functional theory (DFT) was used in the present study.

We have recently demonstrated that clean planar and faceted Ir(2 1 0) are very active and selective to N_2 formation from NO decomposition, with faceted Ir(2 1 0) being more active and selective at higher NO coverage [23]. Here, we report our findings that planar and faceted Ir(2 1 0) show unexpectedly high reactivity for NO decomposition in the presence of pre-adsorbed oxygen. In particular, faceted Ir(2 1 0) exhibits unusually high reactivity for NO decomposition at high fractional oxygen coverage. In addition, we provide evidence for structure sensitivity in adsorption sites and thermal decomposition of NO on O-covered faceted Ir(2 1 0) versus O-covered planar Ir(2 1 0).

2. Experimental and theoretical procedures

TPD and HREELS measurements were conducted in two separate ultra-high vacuum (UHV) systems located at Rutgers University and University of Delaware, respectively [23]. Both UHV systems contain Auger electron spectroscopy (AES), low-energy electron diffraction (LEED), and a quadruple mass spectrometer (QMS). All TPD spectra were acquired at a sample heating rate of ~5 K/s. The HREELS spectrometer (LK 3000) was operated at electron energy of 6.0 eV with a typical resolution between 40 and 60 cm^{-1}. All HREELS spectra were measured in the specular direction at an angle of 60° with the sample held at 130–150 K.

In both TPD and HREELS experiments, the same Ir(2 1 0) crystal was used but different cleaning procedures were applied due to different sample mounting, which give the same planar and faceted Ir(2 1 0) surfaces [23]. At Rutgers University, clean planar Ir(2 1 0) was prepared by cycles of flashing the sample to 1700 K in O_2 (5×10^{-8} Torr) followed by flashing to 1700 K in UHV. Clean faceted Ir(2 1 0) was generated through two steps. In the first step, oxygen-covered faceted Ir(2 1 0) was prepared by annealing clean planar Ir(2 1 0) in O_2 (5×10^{-8} Torr) at 600–1700 K and subsequent cooling in O_2 to 300 K; the average facet size from 5 nm to 14 nm was controlled by the annealing temperature [22]. In the second step, clean faceted Ir(2 1 0) was generated via a reaction with H_2 (5×10^{-9} Torr) at 400 K to remove surface oxygen while facets retained their original structure and size. At University of Delaware, clean planar Ir(2 1 0) was prepared by cycles of Ne^+ sputtering (3 KV and 8–10 μA) and annealing at 700 K in O_2 (5×10^{-8} Torr) to remove surface carbon contamination followed by annealing at 400 K in H_2 (1×10^{-8} Torr) and heating to 700 K in UHV to remove surface oxygen and relax faceted Ir(2 1 0) to planar Ir(2 1 0). Clean faceted Ir(2 1 0) was generated by annealing clean planar Ir(2 1 0) in O_2 (5×10^{-8} Torr) at 600 K for 2 min and subsequent cooling in O_2 to 300 K to form oxygen-covered faceted Ir(2 1 0), which was followed by a reaction with H_2 (1×10^{-8} Torr) at 400 K to remove surface oxygen. This gave rise to clean faceted Ir(2 1 0) with an average facet size of 5 nm [22]. Surface cleanliness was checked using AES and TPD while surface structure was monitored by LEED.

In all experiments, ^{15}NO was used to distinguish $^{15}N_2$ from CO and $^{15}N_2O$ from CO_2 in the TPD measurements. Nitric oxide (^{15}NO), hydrogen (H_2) and oxygen (O_2) are of research purity and were used without further purification; all gases were dosed onto the Ir surfaces at 300 K by backfilling the chambers. NO and oxygen exposures were reported in Langmuir ($1\ L = 10^{-6}$ Torr s) and uncorrected for ion gauge sensitivity. Oxygen coverage expressed in monolayer (ML) for TPD spectra was determined from a oxygen uptake curve obtained on the basis of the integrated area under the TPD spectra of O_2 on Ir(2 1 0) following adsorption at 300 K [21,24], where 1 ML O is defined to be the saturation coverage at ~80 L O_2 dosed on Ir(2 1 0) at 300 K.

To determine energetically favorable binding sites of NO and O on the Ir surfaces for coadsorbed NO and O adlayers, the binding energies of (NO + O) on Ir(2 1 0), Ir(3 1 1) and Ir(1 1 0) with varying adsorption sites of NO and O were calculated by DFT using the CASTEP code [25]. Vanderbilt-type ultrasoft pseudopotentials [26] were applied together with the generalized gradient approximation (GGA) exchange-correlation functional proposed by Perdew, Burke, and Ernzerhof (PBE) [27]. The Ir(2 1 0), Ir(3 1 1) and Ir(1 1 0) surfaces were represented by 16-layer, 11-layer and 12-layer slabs separated by ~12 Å of vacuum, respectively. The bottom three layers for Ir(2 1 0) and Ir(3 1 1) and the bottom four layers for Ir(1 1 0) were fixed at the calculated bulk structures, while the geometries of the remaining layers and the adsorbates were allowed to fully optimize. For all coadsorbed systems of NO and O, a cutoff energy of 340 eV was used and the Brillouin zones of the (1×1) unit cells of Ir(2 1 0), Ir(3 1 1) and Ir(1 1 0) were sampled with 10×8, 14×8, and 14×10 Monkhorst-Pack **k**-point meshes [28], respectively.

3. Results

3.1. TPD Study

Before presenting our TPD spectra from NO on O-covered planar and faceted Ir(2 1 0), we briefly summarize our results of TPD measurements for NO on clean Ir surfaces that are relevant to this work. The detailed description of adsorption and decomposition of NO on clean planar and faceted Ir(2 1 0) have been published elsewhere [23].

At low NO exposure, adsorbed NO undergoes complete decomposition yielding only N_2 as N-containing species on clean planar (<3 L) and faceted (⩽3 L) surfaces of Ir(2 1 0). When both surfaces are saturated by 40 L NO, the dominant desorbing products are large amounts of N_2 and small amounts of NO with traces of N_2O from planar Ir(2 1 0) but no formation of N_2O from faceted Ir(2 1 0). For all NO exposures studied, the formation of NO_2 is not observed and both surfaces are covered by oxygen after TPD which completely desorbs from the surfaces at ~1600 K. Although there are notable differences in the N_2 TPD spectral profiles between the two surfaces, the N_2 peak temperatures from the two surfaces are almost the same. Only a single N_2 peak is observed on the two surfaces with peak temperatures below 560 K.

In the current work, the products monitored during TPD for NO on O-covered planar and faceted Ir(2 1 0) are N_2, NO, N_2O and NO_2, where clean Ir surfaces are first pre-dosed with oxygen and then

exposed to NO prior to heating. For all NO and oxygen exposures studied, no desorption of NO_2 is detected and both surfaces are covered with oxygen after TPD which desorbs totally from the surfaces at ~1600 K. The formation of N_2 signifies direct decomposition of NO on O-covered planar and faceted Ir(2 1 0).

3.1.1. NO on O-covered planar Ir(2 1 0)

Fig. 1 shows a series of TPD spectra of N_2, NO and N_2O from various exposures of NO on planar Ir(2 1 0) pre-dosed to 1 L O_2 (0.5 ML O). No desorption of N_2O is observed, although traces of N_2O are seen for NO on clean planar Ir(2 1 0) at $\geqslant$3 L NO [23], indicating that the formation of N_2O is suppressed in the presence of pre-adsorbed oxygen. For 0.5 L NO, all adsorbed NO decomposes to produce only N_2 with peak temperature below 550 K. For 1 L NO, a new N_2 feature appears as a small shoulder above 600 K together with traces of NO desorption, in addition to the original N_2 peak below 550 K. For NO exposures $\geqslant$2 L, the original N_2 peak below 550 K is dramatically attenuated and the new N_2 feature above 600 K becomes a dominant peak. Simultaneously, a large amount of NO desorbs from the surface, which scales up with NO exposure. Comparison with the TPD spectra from NO on clean planar Ir(2 1 0) [23] leads to the conclusion that the ratio of NO desorption to N_2 desorption here is higher than that on the clean Ir surface [23] for the same NO exposure, which implies that the presence of pre-adsorbed oxygen reduces the surface reactivity for NO decomposition. Notably, the N_2 peak above 600 K in Fig. 1 is not present on clean planar Ir(2 1 0) where N_2 desorbs in a single peak with peak temperature below 560 K [23].

To further examine the effects of pre-adsorbed oxygen on NO decomposition, we have varied oxygen exposure while keeping NO exposure constant. Fig. 2a shows TPD spectra of N_2 and NO from 1 L NO on planar Ir(2 1 0) pre-covered with various amounts of oxygen. We note that no desorption of N_2O is seen. In the absence of pre-adsorbed oxygen, adsorbed NO decomposes totally to evolve only N_2 with peak temperature below 550 K. When the surface is pre-covered by 0.3 ML O, NO also totally decomposes to produce only N_2 and the position of the N_2 peak (P1) remains the same as that on the clean surface. As oxygen coverage increases, the intensity of the original N_2 peak (P1) is attenuated gradually and a new N_2 feature develops on the high temperature side (initially a shoulder and finally a peak "P2" with peak temperature located above 600 K), which is accompanied by NO desorption that increases with oxygen coverage. When the surface is pre-covered with 1 ML O, no formation of N_2 is detectable and all adsorbed NO desorbs without dissociation; NO decomposition is completely suppressed. As NO exposure increases to 2 L (Fig. 2b), the intensity of the N_2 peak on the clean surface increases compared to 1 L NO: the integrated N_2 area from 2 L NO is about twice of that from 1 L NO. With pre-adsorbed oxygen, a similar new N_2 feature on the high temperature side (initially a shoulder and finally a peak) is also observed, which is visible at 0.3 ML O together with a reduction of the original N_2 peak and emergence of NO desorption. It is noted that the shoulder of the new N_2 feature here appears at lower oxygen coverage compared to that for 1 L NO in Fig. 2a. At 0.7 ML O, only a small amount of adsorbed NO decomposes and adsorbed NO mainly desorbs molecularly.

3.1.2. NO on O-covered faceted Ir(2 1 0)

TPD spectra of N_2 and NO from different exposures of NO on faceted Ir(2 1 0) (with average facet size ~14 nm) pre-dosed to 1 L O_2 (0.5 ML O) are presented in Fig. 3. No evidence for the formation of N_2O is found. For NO exposures $\leqslant$2 L, adsorbed NO entirely decomposes to form N_2. For NO exposure $\geqslant$3 L, NO desorption is visible which increases with NO exposure while the desorption of N_2 progressively broadens but no peak above 600 K develops, in contrast

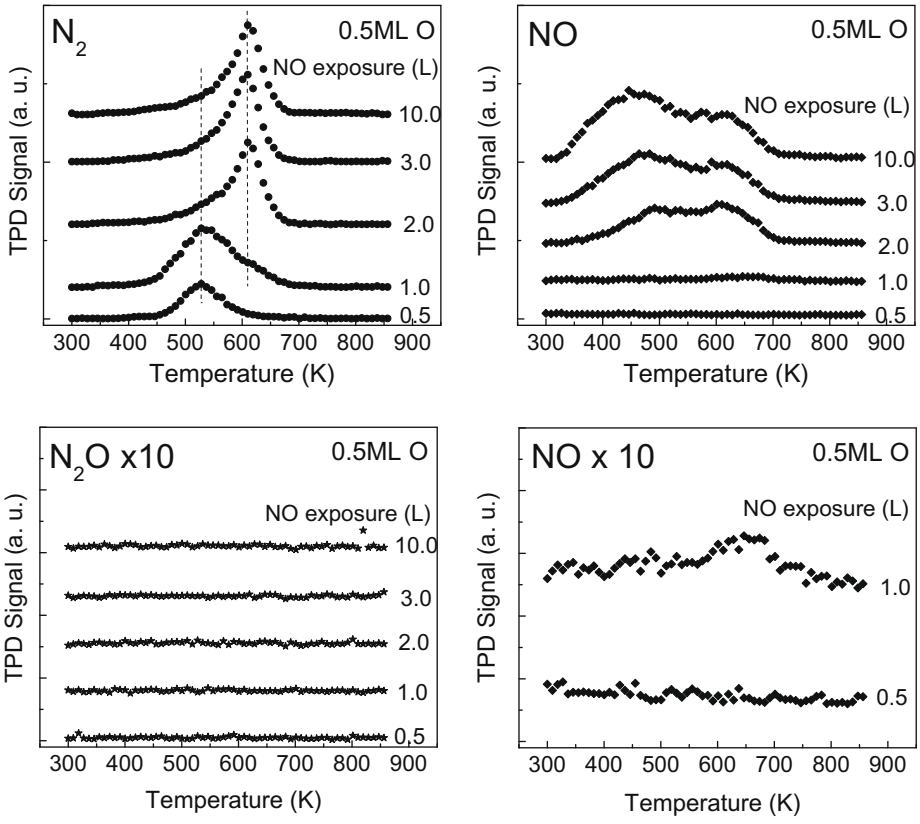

Fig. 1. TPD spectra of N_2, NO and N_2O from different exposures of NO on planar Ir(2 1 0) pre-dosed to 1 L O_2 (0.5 ML O).

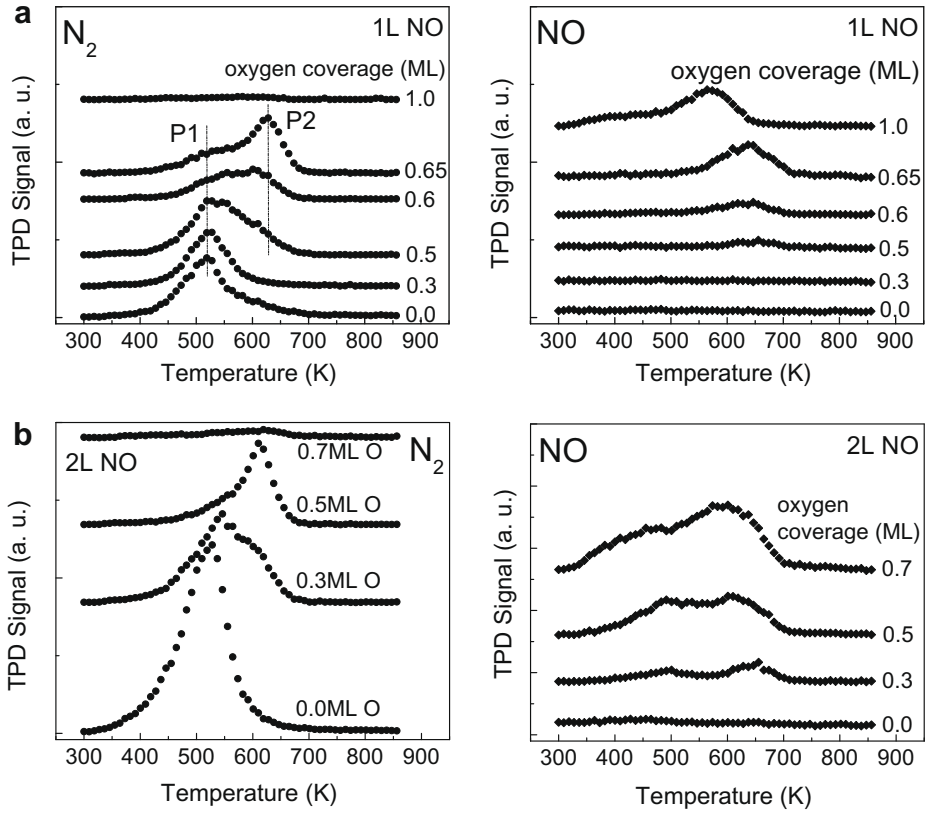

Fig. 2. TPD spectra of N_2 and NO from NO on planar Ir(2 1 0) pre-covered with various amount of oxygen. (a) 1 L NO; (b) 2 L NO.

to NO on 0.5 ML O-covered planar Ir(2 1 0) shown in Fig. 2a where a new peak grows above 600 K.

Fig. 4 displays TPD spectra of N_2 and NO from 2 L NO on faceted Ir(2 1 0) as a function of pre-adsorbed oxygen coverage. No evidence for the formation of N_2O is found. In the absence of pre-adsorbed oxygen, only a narrow intense N_2 peak is seen, indicative of complete decomposition of NO. When the surface is pre-covered by 0.5 ML O, NO also completely decomposes to give rise to only N_2 and the position of the N_2 peak (F1) remains the same. At 0.65 ML O, a new N_2 feature develops as a shoulder above 600 K together with the reduction of the original N_2 peak (F1), which is accompanied by NO desorption. Further increasing oxygen coverage to 0.7 ML O, the original N_2 peak (F1) diminishes and the new N_2 feature becomes an evident peak (F2) and NO desorption further increases. When the surface is pre-covered with 1 ML O, adsorbed NO desorbs without dissociation; NO decomposition is entirely inhibited.

Fig. 5 compares the TPD spectra of N_2 and NO from 2 L NO on O-covered faceted Ir(2 1 0) (with average facet size ~14 nm) with those on O-covered planar Ir(2 1 0). At 0.3 ML O, both surfaces exhibit high activity in NO decomposition. N_2 desorbs in a single peak (F1) from faceted Ir whereas N_2 appears in two peaks (P1 and P2) from planar Ir. No desorption of NO from faceted Ir is observed, indicating complete decomposition of NO although small amount of NO desorbs from planar Ir. At 0.5 ML O, both surfaces are still active for NO decomposition, which is in contrast to Ir(1 0 0) on which 0.5 ML O completely suppresses NO decomposition [17]. Moreover, the intensity of the N_2 peak "P1" drastically reduces and the intensity of the N_2 peak "P2" increases while the peak temperature of the N_2 feature from the faceted Ir (F1) does not change, compared to 0.3 ML O. Although NO desorption from planar Ir increases, there is still no desorption of NO from faceted Ir, i.e. NO dissociates entirely on faceted Ir. At 0.7 ML O, planar Ir has little activity whereas faceted Ir still remains active in NO decomposition. This is evidenced by dominant NO desorption with traces of N_2 desorption from planar Ir but much more N_2 desorption (comparable to NO desorption) from faceted Ir. The unusually high reactivity of faceted Ir for NO decomposition at such high fractional oxygen coverage is a surprising result. Notably, the original N_2 peak (F1) disappears and a new N_2 peak (F2) on the high temperature side with peak temperature above 600 K develops together with NO desorption from faceted Ir. The striking differences in desorption of N_2 and NO between O-covered planar and faceted Ir(2 1 0) provide evidence for strong structure sensitivity in NO decomposition with faceted Ir(2 1 0) being more active than planar Ir(2 1 0). It is worth mentioning that previous TPD measurements from CO on O-covered planar and faceted Ir(2 1 0) have indicated that planar Ir(2 1 0) exhibits higher reactivity for oxidation of CO than faceted Ir(2 1 0) [24].

To search for facet size effects in NO decomposition on O-covered faceted Ir(2 1 0), we have measured TPD spectra from NO on O-covered faceted Ir(2 1 0) with different facet sizes (5 and 14 nm). No formation of N_2O is observed from the two faceted surfaces, indicating no change in selectivity to N_2 formation for NO decomposition. The TPD spectra of N_2 and NO from the two faceted surfaces appear to be very similar in terms of spectra profile, peak position and peak intensity (spectra not shown), implying no change in reactivity for NO decomposition either. All these similarities indicate that on the O-covered faceted Ir(2 1 0) NO decomposition is insensitive to the facet size in NO decomposition, similar to oxidation of CO on O-covered faceted Ir(2 1 0) [24]. The absence of facet size effects in NO decomposition over O-covered faceted Ir(2 1 0) containing (1 1 0) and {3 1 1} facets suggests that the edge and corner atoms between the boundaries of the facets, which increase in concentration as facet size decreases, are not as significant for this process as are the planar microfacets on the facet

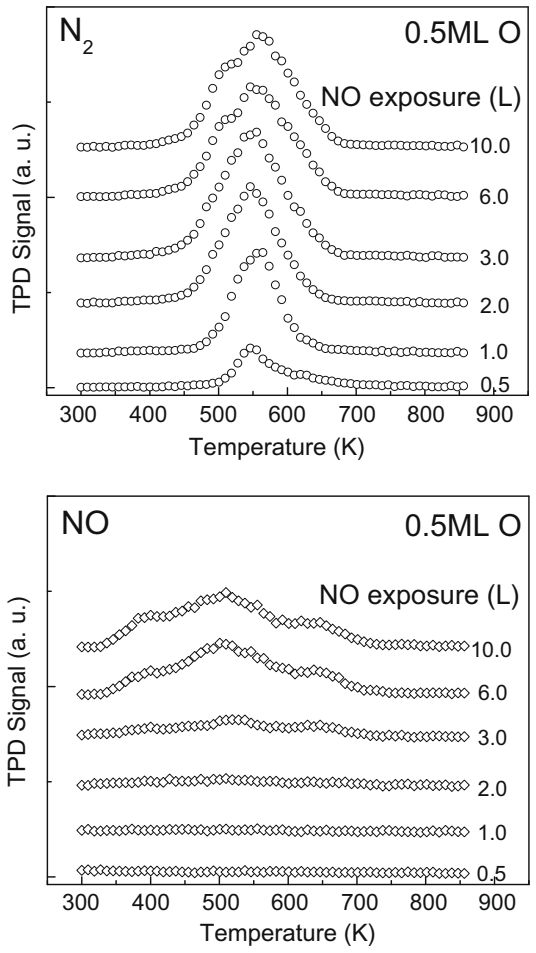

Fig. 3. TPD spectra of N_2, NO and N_2O from different exposures of NO on faceted Ir(2 1 0) pre-dosed to 1 L O_2 (0.5 ML O).

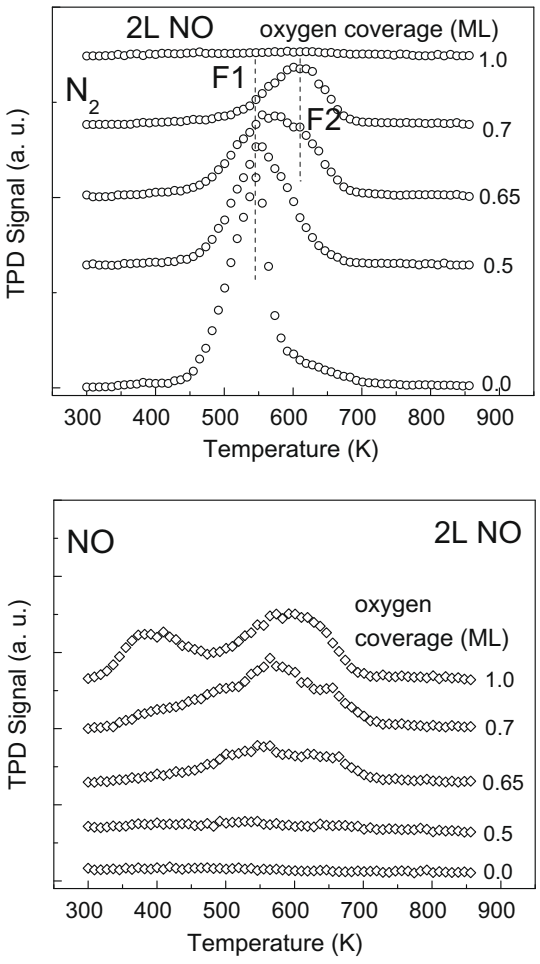

Fig. 4. TPD spectra of N_2 and NO from 2 L NO on faceted Ir(2 1 0) pre-covered with different amount of oxygen.

planes, where {3 1 1} consist of both (1 1 1) and (1 0 0) microfacets [29].

3.2. HREELS Study

Fig. 6a shows the HREEL spectrum from adsorption of 2 L NO on planar Ir(2 1 0) pre-dosed to 1 L O_2 at 300 K. Only a single N–O stretching loss feature, ν(N–O), is observed at 1790 cm^{-1}. This N–O stretching frequency is assigned to the N–O stretching vibration for NO on the atop sites of Ir(2 1 0) based on a comparison with the characteristic N–O stretching feature of atop bound NO on clean Ir and other meal surfaces [23]. The assignment is also supported by our DFT calculations, which will be described in Section 3.3. The frequency of ν(N–O) is slightly higher than that on the clean surface [23], indicative of slight N–O bond strengthening induced by the presence of pre-adsorbed oxygen. Fig. 6b shows the HREEL spectrum from adsorption of 2 L NO on faceted Ir(2 1 0) pre-dosed to 1 L O_2 at 300 K. Two N–O stretching loss features, ν_1(N–O) and ν_2-(N–O), at 1600 cm^{-1} and 1770 cm^{-1}, respectively, are observed in contrast to that on the planar surface, indicating structure sensitivity in adsorption sites of NO. These two N–O stretching modes,ν_1(N–O) and ν_2(N–O), on faceted Ir(2 1 0) are assigned to the stretching vibration of NO on bridge and atop sites of Ir(1 1 0) and {3 1 1} faces on faceted Ir(2 1 0), respectively. The assignments are based on a comparison with the characteristic N–O stretching features of bridge and atop bound NO on clean Ir and other meal surfaces [23]. The assignments are also supported by our DFT calculations, which will be described in Section 3.3. The frequencies of ν_1(N–O) and ν_2(N–O) are slightly higher than those on the clean surface [23], indicating slight N–O bond strengthening induced by pre-adsorbed oxygen. The vibrational feature for CO (~2000 cm^{-1}) is due to background gas adsorption.

3.3. DFT study

First, we briefly summarize our DFT investigations on adsorption sites of O and NO on Ir, respectively, which have been published elsewhere [23,30]. Fig. 7 shows the possible adsorption sites for adsorbate on Ir(2 1 0), Ir(1 1 0) and Ir(3 1 1), respectively. In Fig. 8a and b, we have labeled the energetically favorable binding sites of O (red[2] circles) and NO (blue hexagons) on the different Ir surfaces based on an adsorbate coverage of 1 GML O and 1 GML NO, respectively, where 1 GML refers to one geometrical monolayer and is defined as one O or NO per (1x1) surface unit cell. The corresponding binding energies (BEs) are summarized in Table 1. In the case of O on Ir (Fig. 8a), O prefers to bind on atop (T), bridge (D and C) and hollow (B) sites of Ir(2 1 0) with similar binding energies (1.74–1.78 eV) but only on bridge sites of Ir(1 1 0) (D) and Ir(3 1 1) (A) [30]. As for NO on Ir (Fig. 8b), NO binds most strongly on the atop (T) sites of Ir(2 1 0) while on both atop and bridge sites of Ir(1 1 0) (T and D) and Ir(3 1 1) (A and T) [23].

DFT calculations on coadsorption of (NO + O) on Ir(2 1 0), Ir(1 1 0) and Ir(3 1 1) have been performed for one NO molecule

[2] For interpretation of color in Fig. 8, the reader is referred to the web version of this article.

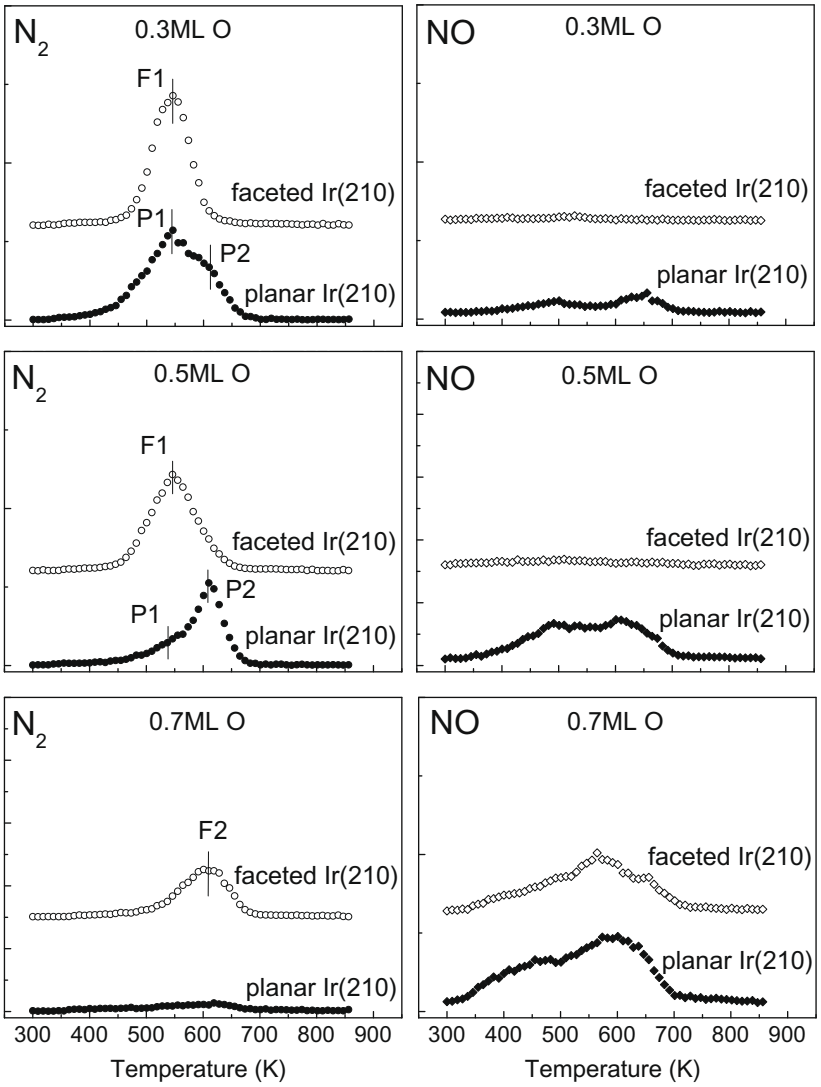

Fig. 5. TPD spectra of N_2 and NO from 2 L NO on planar and faceted Ir(2 1 0) pre-covered by 0.3 ML O, 0.5 ML O and 0.7 ML O, respectively.

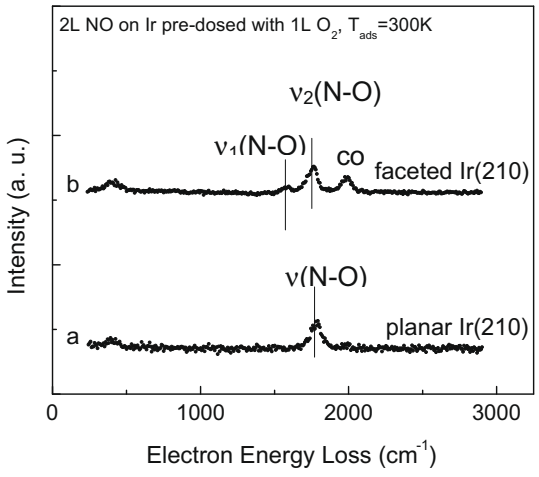

Fig. 6. HREEL spectra following the adsorption of 2 L NO on planar and faceted Ir(2 1 0) pre-dosed with 1 L O_2 at 300 K.

plus one O atom per (1×1) unit cell at different combinations of adsorption sites. Among the different overlayers, Fig. 8c and Table 1 summarize the energetically favorable binding sites and overall binding energies of coadsorbed NO and O on the three different Ir surfaces.

On Ir(2 1 0) the most stable coadsorption system is the one where NO binds on atop (T) sites while O binds on bridge (D) sites. Apparently, on Ir(2 1 0) both adsorbates are able to occupy their preferred binding sites, without showing major site blocking effects. The overall binding energy of this system is 3.55 eV, which is 1.16 eV smaller than the sum of the binding energies of both homonuclear (and independent) adsorbate systems (1.76 eV + 2.95 eV). This finding supports our HREELS data for NO on O-covered planar Ir(2 1 0) where only atop bound NO is observed as described in Section 3.2.

On Ir(1 1 0) the coadsorption system with NO on short-bridge (D) sites and O on long-bridge (C) sites is energetically preferred with an overall binding energy of 2.11 eV. In contrast to Ir(2 1 0), now site blocking effects play a role since both adsorbates prefer binding at the short-bridge (D) sites when they are alone on the surface. Since NO shows a ~0.7 eV stronger interaction with Ir(1 1 0) than O does, NO occupies D sites, forcing O to the C sites. With this combination of adsorption sites (C + D), the overall binding energy of 2.11 eV is even below the value for only NO adsorbed on Ir(1 1 0) (BE = 2.31 eV).

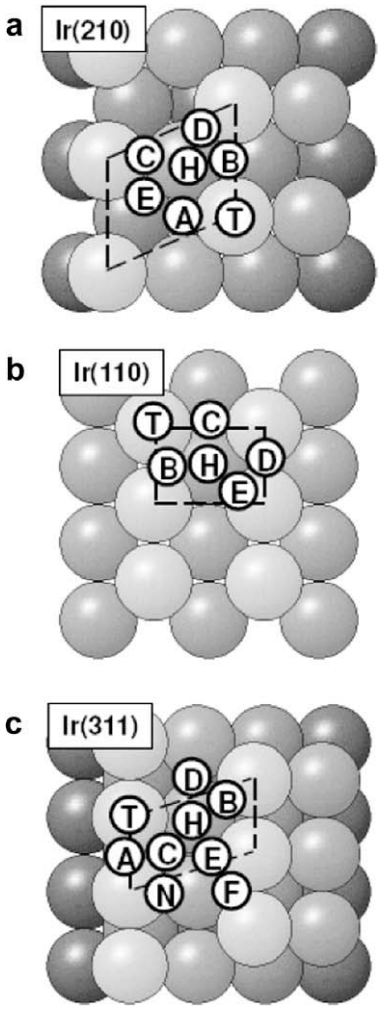

Fig. 7. Top views of hard-sphere bulk truncation models of Ir(2 1 0), Ir(1 1 0) and Ir(3 1 1) showing possible adsorption sites for adsorbate.

Finally, on Ir(3 1 1) there are three energetically almost degenerate coadsorption systems: a) "A+N" combination of NO on bridge (A) sites and O on bridge (N) sites with an overall BE of 2.78 eV; b) "A + E" combination of NO on bridge (A) sites and O on hollow (E) sites with an overall BE of 2.70 eV; c) "T + N" combination of NO on atop (T) sites and O on bridge (N) sites with an overall BE of 2.69 eV. Although the "A + N" combination is slightly favored compared to the other overlayers, all might be relevant due to the small energy differences. Therefore, one can conclude that on Ir(3 1 1) NO binds on bridge (A) and atop (T) sites while O binds on bridge (N) and hollow (E) sites. Similar to (NO + O) on Ir(1 1 0), site blocking effects are observed here.

Taking the DFT data for (NO + O)/Ir(1 1 0) and (NO + O)/Ir(3 1 1) together, the calculations support the HREELS results for NO on O-covered faceted Ir(2 1 0) comprising (1 1 0) and {3 1 1} faces, where both bridge and atop bound NO species are observed as described in Section 3.2.

Careful examination of adsorption sites and BE values for NO [23], O [30] and (NO + O) on Ir(2 1 0), Ir(1 1 0) and Ir(3 1 1) leads to the following conclusions. (1) Coadsorption of O does not influence adsorption sites of NO but reduces Ir-NO bond strength on Ir(2 1 0), Ir(1 1 0) and Ir(3 1 1); (2) in contrast, coadsorption of NO indeed influences adsorption sites of O and reduces Ir–O bond strength on Ir(1 1 0) and Ir(3 1 1) significantly.

4. Discussion

In an earlier study by Yates and Madey, kinetic evidence indicated that catalytic dissociation of NO occurs through the interaction of an adsorbed NO molecule with a neighboring empty site [31]. In order to better fit experimental kinetic parameters, Borg et al. have modified the rate equation by including an ensemble of several vacant sites for dissociation of a single NO molecule [32]. Our data of NO decomposition on clean [23] and O-covered planar and faceted Ir(2 1 0) are consistent with the conclusion that vacant sites are involved in the activation step for decomposition of NO, where adsorbed NO on a vertical binding configuration via N atom at 300 K may interconvert to a lying-down binding configuration via N and O atoms at elevated temperature, which is a precursor for the N–O bond breaking. The requirement of an ensemble of vacant sites is consistent with the observation that adsorbed NO undergoes complete decomposition on clean and O-covered planar and faceted Ir(2 1 0) only in the limit of low NO and oxygen coverage as well as the absence of size effects in NO decomposition on faceted Ir(2 1 0) with and without pre-adsorbed oxygen.

The TPD data have revealed pronounced changes in the N_2 spectra from NO on O-covered planar and faceted Ir(2 1 0) (<1 ML O) as compared to those on the clean surfaces, demonstrating that the presence of pre-adsorbed oxygen strongly influences the thermal decomposition of NO. The prominent new feature of the N_2 spectra in the presence of pre-adsorbed oxygen is the development of N_2 peak above 600 K ("P2" and "F2" in Fig. 5, denoted hereafter as the β-state) accompanied by NO desorption, in addition to the appearance of N_2 peak below 550 K ("F1" and "P1" in Fig. 5, denoted hereafter as α-state) that is also observed on the clean surfaces. It is found that the α-state N_2 appears and dominates at lower oxygen coverage with the same or similar peak temperature as that on the clean surfaces, suggesting that the α-state N_2 is produced in the similar way as that on the clean surfaces at low NO coverage. The observation of the β-state N_2 appearing and dominating at higher fractional oxygen coverage accompanied by NO desorption indicates that the β-state N_2 is formed on the area of the surfaces that has to be freed up by NO desorption prior to NO dissociation. Therefore, we propose that the two N_2 peaks from NO on O-covered planar and faceted Ir(2 1 0) are attributed to NO dissociation on two different types of environments. The α-state N_2 originates from NO dissociation on the "open" area with available ensembles of vacant sites. Whereas the β-state N_2 originates from NO dissociation on the "filled" area occupied by NO and pre-adsorbed O atoms so that some adsorbed NO molecules have to desorb first from the surfaces in order to create ensembles of empty sites required for NO dissociation. The observation that the β-state N_2 peak from faceted Ir (F2) appears at higher fractional oxygen coverage than that from planar Ir (P2) can be correlated to the higher density of "open" area on the faceted surface compared to that on the planar surface for the same condition.

Both experiments and calculations have demonstrated that the low-coordinated surface metal atoms of atomic steps are the most active sites for NO dissociation on hcp Ru surfaces [33–35]. Similarly, studies of NO on fcc metal surfaces show that open surfaces containing low coordination sites of C_6 or C_7 are much more active compared to the more close-packed surfaces without such low coordination sites [23,36–38]; C_6 or C_7 denotes the six or seven nearest-neighbor metal atoms. Especially, recent DFT calculations performed by Inderwildi et al [13,14] illustrate that the activation barrier for NO dissociation is lower on Rh(3 1 1) than Rh(1 1 1) on both clean and O-covered Rh surfaces, although the activation barrier increases with pre-adsorbed oxygen coverage on each Rh surface. In addition, their calculations indicate that the difference in the activation barrier for NO dissociation on Rh(3 1 1) and

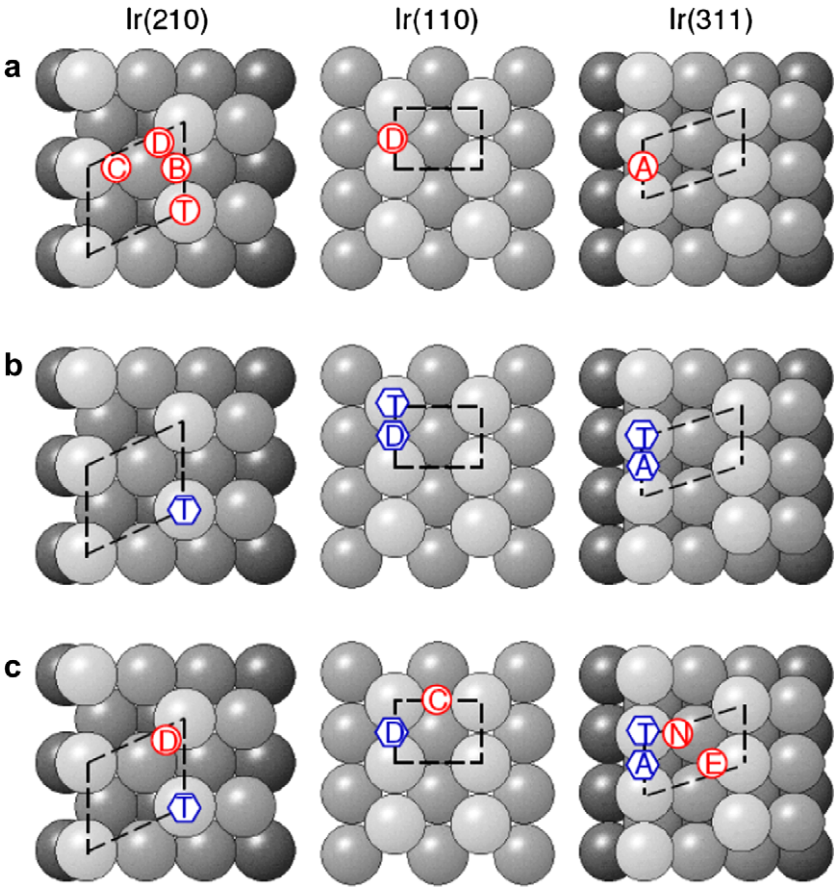

Fig. 8. Top views of hard-sphere bulk truncation models of Ir(2 1 0), Ir(1 1 0) and Ir(3 1 1) showing energetically favorable binding sites for O (a), NO (b) and O + NO (c).

Table 1
Binding sites and binding energies (BEs) for O, NO, and O + NO on Ir(2 1 0), Ir(1 1 0) and Ir(3 1 1) surfaces where one O or one NO or one NO plus one O per (1×1) unit cell was used in the calculations.

Ir(2 1 0)			Ir(1 1 0)			Ir(3 1 1)		
	O	BE (eV)		O	BE (eV)		O	BE (eV)
	C	−1.75		C	−0.68		E	−0.68
	B	−1.74		H	−0.29		N	−1.14
	T	−1.78		D	−1.59		A	−1.72
	D	−1.76		T	−1.10		T	−1.18
				E	−0.61		F	−1.30
NO		BE (eV)	NO		BE (eV)	NO		BE (eV)
T		−2.95	D		−2.31	A		−2.51
C		−2.42	T		−2.35	T		−2.34
NO	O	BE (eV)	NO	O	BE (eV)	NO	O	BE (eV)
T	C	−3.26	D	C	−2.11	A	E	−2.70
T	H	−2.64	D	H	−0.62	A	N	-2.78
C	B	−2.48	T	C	−1.36	T	N	−2.69
C	T	−2.61	T	H	−0.78			
T	D	−3.55						

Rh(1 1 1) in the absence and presence of pre-adsorbed oxygen is mainly attributed to the steric effects induced by the structural differences. Thus, the higher reactivity of O-covered planar Ir(2 1 0) in the current study could be attributed to the presence of low-coordination C_6 sites on Ir(2 1 0), compared to that of O-covered Ir(1 0 0) where 0.5 ML O completely suppresses NO decomposition [17]. The higher reactivity of O-covered faceted Ir(2 1 0) than that of planar Ir(2 1 0) may be associated with weaker Ir–O bond strength indicated in our DFT calculations and the presence of nanometer scale features on the faceted surface. As indicated in Section 3.3, the O binding energy on Ir(1 1 0) and Ir(3 1 1) is reduced and significantly lower than that on planar Ir(2 1 0), which may facilitate pre-adsorbed O atoms to diffuse, recombine and desorb from the surface prior to NO dissociation. As discussed previously, nanoscale pyramids on faceted Ir(2 1 0) provide favorable condition for reaction coupling between different facets, leading to unusually high reactivity of faceted Ir(2 1 0) for N–O bond breaking [23]. Kinetic simulations of catalytic reaction of $2A + B_2 \rightarrow 2AB$ on supported nanoscale catalyst particles indicate that the reaction kinetics on a faceted nanocrystal can be remarkably different from those on a single crystal surface due to interplay of the reaction kinetics on different facets of supported particles [39]. Similar studies of Monte Carlo simulations for the dissociation of NO on O-covered faceted Ir(2 1 0) are necessary to elucidate the role of nanometer scale features in the unusually high reactivity of O-covered faceted Ir(2 1 0) toward NO decomposition.

In the above discussion, the nature of the low-coordinated surface atoms is not considered. As a matter of fact, the local geometric structures around these low-coordinated atoms are also important for N–O bond breaking. Using DFT calculations, Ge and Neurock have identified an ensemble of square-arranged Pt atoms as an important feature in activating the N–O bond on Pt surfaces [40]. The detailed characterization of NO dissociation on O-covered planar and faceted Ir(2 1 0) by means of DFT calculations and scanning tunneling microscopy (STM) will be the subject of future study to gain insights into the nature of active sites for NO dissociation on O-covered planar and faceted Ir(2 1 0).

It should be noted that phase separation into pure adsorbate islands often occurs for coadsorbed overlayer on metal surfaces. Using LEED IV analysis, it has been found that CO and O form sep-

arated islands when CO is adsorbed on O-covered Ir(1 0 0) [41] and Pd(1 1 1) [42], which is related to the large energy difference for CO adsorption on different adsorption sites of the bare surface [42]. In STM studies of NO on O-covered Rh(1 1 1) [12], NO and O form separate islands that depend strongly on the initial adsorbate coverage and adsorption temperature. In particular, the formation of NO islands is very sensitive to the O coverage prior to NO adsorption, and NO islands are only observed at O coverage between 0.15 and 0.23 ML O [12]. STM studies or LEED IV analysis of NO on O-covered planar and faceted Ir(2 1 0) would be needed to provide evidence whether NO and O form separate phases or mixed phase upon adsorption and after annealing to elevated temperatures.

5. Conclusion

We find clear evidence for structure sensitivity in adsorption sites and thermal decomposition of NO on faceted Ir(2 1 0) versus planar Ir(2 1 0), pre-dosed with oxygen. No size effects in the thermal decomposition of NO on O-covered faceted Ir(2 1 0) is observed for an average facet size from 5 to 14 nm, which suggests that the edge and corner atoms between the boundaries of the facets are not as significant for N–O bond breaking as are the planar microfacets within the facet planes. The presence of pre-adsorbed oxygen suppresses the formation of N_2O and reduces the surface reactivity for NO decomposition. In the presence of pre-adsorbed oxygen, a new N_2 peak develops above 600 K accompanied by NO desorption on both surfaces, in addition to the appearance of a N_2 peak observed also on the clean surfaces. The observation that the N_2 peak above 600 K appears at higher fractional oxygen coverage on faceted Ir(2 1 0) than that on planar Ir(2 1 0) correlates with higher reactivity of faceted Ir(2 1 0) for NO decomposition at higher fractional oxygen coverage.

Acknowledgment

Discussions with Dr. Q. Shen and Dr. H. Wang are greatly appreciated. The Rutgers University authors acknowledge support from the US Department of Energy, Office of Basic Energy Sciences (Grant No. DE-FG02-93ER14331). The University of Delaware authors acknowledge support from the US Department of Energy, Office of Basic Energy Sciences (Grant No. DEFG02-00ER15104). P.K. and T.J. gratefully acknowledge support by the German Academic Exchange Service (DAAD) and the Deutsche Forschungsgemeinschaft (DFG) within the Emmy-Noether-Program.

References

[1] R. Burch, P.J. Millington, Catal. Today 29 (1996) 37.
[2] C. Márquez-Alvarez, I. Rodríguez-Ramos, A. Guerrero-Ruiz, G.L. Haller, M. Fernández-García, J. Am. Chem. Soc. 119 (1997) 2905.
[3] R. Burch, J.P. Breen, F.C. Meunier, Appl. Catal. B 39 (2002) 283.
[4] M.D. Amiridis, C. Mihut, M. Maciejewski, A. Baiker, Topics Catal. 28 (2004) 141.
[5] P. Vernoux, F. Gaillard, R. Karoum, A. Billard, Appl. Catal. B 73 (2007) 73.
[6] N. Jagtap, S.B. Umbarkar, P. Miquel, P. Granger, M.K. Dongare, Appl. Catal. B 90 (2009) 416.
[7] V.I. Pârvulescu, P. Grange, B. Delmon, Catal. Today 46 (1998) 233.
[8] C. Nyberg, P. Uvdal, Surf. Sci. 256 (1991) 42.
[9] R.J. Mukerji, A.S. Bolina, W.A. Brown, Surf. Sci. 547 (2003) 27.
[10] J.B. Li, W.X. Huang, Z.Q. Jiang, X.H. Bao, Chinese J. Catal. 27 (2006) 65.
[11] T.W. Root, L.D. Schmidt, G.B. Fisher, Surf. Sci. 134 (1983) 30.
[12] H. Xu, K.Y.S. Ng, Surf. Sci. 365 (1996) 779.
[13] O.R. Inderwildi, D. Lebiedz, O. Deutschmann, J. Warnatz, J. Chem. Phys. 122 (2005) 154702.
[14] O.R. Inderwildi, D. Lebiedz, O. Deutschmann, J. Warnatz, ChemPhysChem 6 (2005) 2513.
[15] B.E. Hayden, K. Kretzschmar, A.M. Bradshaw, Surf. Sci. 125 (1983) 366.
[16] Z.-P. Liu, S.J. Jenkins, D.A. King, J. Am. Chem. Soc. 126 (2004) 10746.
[17] S. Khatua, G. Held, D.A. King, Surf. Sci. 586 (2005) 1.
[18] J.G. Chen, W. Erley, H. Ibach, Surf. Sci. 224 (1989) 215.
[19] F. Bozso, J. Arias, C.P. Hanrahan, J.T. Yates, R.M. Martina, H. Metiu, Surf. Sci. 141 (1984) 591.
[20] W. Chen, I. Ermanoski, Q. Wu, T.E. Madey, H.H. Hwu, J.G. Chen, J. Phys. Chem. B 107 (2003) 5231.
[21] I. Ermanoski, K. Pelhos, W. Chen, J.S. Quinton, T.E. Madey, Surf. Sci. 549 (2004) 1.
[22] W. Chen, I. Ermanoski, T.E. Madey, J. Am. Chem. Soc. 127 (2005) 5014.
[23] W. Chen, T.E. Madey, A.L. Stottlemyer, J.G. Chen, P. Kaghazchi, T. Jacob, J. Phys. Chem. C 112 (2008) 19113.
[24] W. Chen, I. Ermanoski, T. Jacob, T.E. Madey, Langmuir 22 (2006) 3166.
[25] M.D. Segall, P.J.D. Lindan, M.J. Probert, C.J. Pickard, P.J. Hasnip, S.J. Clark, M.C. Payne, J. Phys. Conden. Matt. 14 (2002) 2717.
[26] D. Vanderbilt, Phys. Rev. B 41 (1990) 7892.
[27] J.P. Perdew, K. Burke, M. Ernzerhof, Phys. Rev. Lett. 77 (1996) 3865.
[28] H.J. Monkhorst, J.D. Pack, Phys. Rev. B 13 (1976) 5188.
[29] R. Apel, D. Farías, H. Tröger, K.H. Rieder, Surf. Sci. 331–333 (1995) 57.
[30] P. Kaghazchi, T. Jacob, I. Ermanoski, W. Chen, T.E. Madey, ACS Nano 2 (2008) 1280.
[31] J.T. Yates Jr, T.E. Madey, J. Chem. Phys. 45 (1966) 1623.
[32] H.J. Borg, J.F.C.-J.M. Reijerse, R.A.V. Santen, J.W. Niemantsverdriet, J. Chem. Phys. 101 (1994) 10052.
[33] T. Zambelli, J. Wintterlin, J. Trost, G. Ertl, Science 273 (1996) 1688.
[34] F. Garin, Appl. Catal. A 222 (2001) 183.
[35] B. Hammer, Phys. Rev. Lett. 83 (1999) 3681.
[36] L.A. DeLouise, N. Winograd, Surf. Sci. 159 (1985) 199.
[37] I. Nakamura, T. Fujitani, H. Hamada, Surf. Sci. 514 (2002) 409.
[38] S. Sugai, K. Takeuchi, T. Ban, H. Miki, K. Kawasaki, T. Kioka, Surf. Sci. 282 (1993) 67.
[39] V.P. Zhdanov, B. Kasemo, Surf. Sci. Rep. 39 (2000) 25.
[40] Q. Ge, M. Neurock, J. Am. Chem. Soc. 126 (2004) 1551.
[41] T.J. Lerotholi, G. Held, D.A. King, Surf. Sci. 601 (2007) 1285.
[42] A.P. Seitsonen, Y.D. Kim, S. Schwegmann, H. Over, Surf. Sci. 468 (2000) 176.